

Free space path loss is a function of frequency and propagation distance and the RF signal propagates at light speed in all directions in free space. The performance evaluation of wireless and radar communication technologies is related to understanding the propagation environments. This work presents the modeling of several RF propagation properties that include atmospheric attenuation due to rain, free space path loss, gas, and fog, as well as multipath propagations caused by ground bounces. The methodology discusses the developed model according to the series of (ITU) International Telecommunication Union references to radio wave propagation. This work discusses the Free Space Path Losses (FSPL), and Propagation Losses (PL) due to the atmosphere, precipitation, snow, rain, clouds, fog, atmospheric lensing and absorption, and polarization mismatch. The work also discusses the vertical coverage diagram and radar propagation factor. The obtained results demonstrate that the PL increases with frequency and range, at a 90-degree roll angle, the attenuation approaches infinity, and as the altitude rises, the amount of attenuation caused by lensing decreases. The analysis of attenuation at 1 km vs. frequency variations, at roughly 60 GHz, indicated a high absorption owing to air gas. Lensing attenuations are also offered as secondary outputs for convenience, the wideband channels present higher performance crossways and a wide range of target height as expected. When the target height increases, the influence of multi-path fading approximately vanishes entirely due to the variation increasing in the spreading delay between the bounce and direct pathway signals. This will reduce the coherence sum between these two samples on receiving by the target

Keywords: free space path loss (FSPL), propagation losses (PL), weather antenna attenuation

IDENTIFYING SOME REGULARITIES OF RADIO FREQUENCY PROPAGATION OF A RADAR SYSTEM BY ANALYZING DIFFERENT ENVIRONMENTAL EFFECTS

Ekhlas Kadhum Hamza

Doctor of Electric Engineering/Communications
Department of Control and Systems Engineering*

Sameir A. Aziez

Doctor of Communication Engineering
Department of Electromechanical Engineering*

Ahmed Hameed Reja

Doctor of Communication Engineering
Department of Electromechanical Engineering*

Ahmad H. Sabry

Corresponding author
Doctor of Control and Automation Engineering
Department of Computer Engineering
Al-Nahrain University

Al Jadriyah Bridge, Baghdad, Iraq, 64074

E-mail: ahs4771384@gmail.com

*University of Technology – Iraq

Al-Sina'a str., Baghdad, Iraq, 10066

Received date 15.07.2022

Accepted date 28.09.2022

Published date 27.10.2022

How to Cite: Hamza, E. K., Aziez, S. A., Reja, A. H., Sabry, A. H. (2022). Identifying some regularities of radio frequency propagation of a radar system by analyzing different environmental effects. *Eastern-European Journal of Enterprise Technologies*, 5 (9 (119)), 61–67. doi: <https://doi.org/10.15587/1729-4061.2022.264093>

1. Introduction

RADAR is referred to as radio detection and ranging as it uses radio signals for detecting and finding the range of a target. It sends radio signals to the target and these radio signals get reflected on the radar. It analyzes these signals and based on that can detect that there is some target located at a particular place and what is its range velocity and angle. It was first used in 1942 and that was the time of World War II by the US. It sends electromagnetic radio waves to any distant object and then it analyzes the reflected waves or the echo signal of the target. Radars can detect moving and static targets and can find the range angle and velocity of the target [1]. Radars provide superior penetration ability throughout any kind of climate circumstances like snow, fog, and rain.

To simulate a radar system, simulation reliability of results relies not only on target and radar models but also on the environment models of the radio frequency (RF) [2, 3]. This includes diffraction [4, 5], multipath [6], and clutter [2]. All of these parameters can only provide inadequate data on radar models and can be analyzed as a pattern-propagation parameter of the RF signal. Radar modeling requires simulating signal echoes and must include information like polarization [7], Doppler frequency, phase shift, delay, etc. By analyzing and discussing the algorithms and principles of ground effects RF environments, it is possible to offer reliable RF environments to simulate radar signal levels.

The Cramér-Rao lower bound is used to investigate antenna properties over a mono-static multiple-input-multiple-output (MIMO) radar for target tracking techniques [8]. This type of radar was developed for multi-band MIMO

systems and is in the form of a practical antenna array. Understanding the propagation environment is essential for evaluating wireless communication and radar systems. Applications that can benefit from developing radio frequency propagation of a radar system are given in [9, 10].

A statistical model with average features is used to model the propagation environment [11–13]. A propagation model, in general, is made up of three parts: a rapid fading, shadow fading, and path loss-dependent component as shown in Fig. 1. Traditional 2-dimensional (2D) propagation models (Fig. 1, *a*) consider only the base station, the distance between the UE, and the azimuth angle. However, in recent years, 3-dimensional (3D) models have been more popular than considering both the elevation and azimuth angles of the UE to effectively predict the impact of antenna down tilt as shown in Fig. 1, *b*. Therefore, understanding the propagation environment is important for correctly evaluating the performance of wireless communication and radar devices.

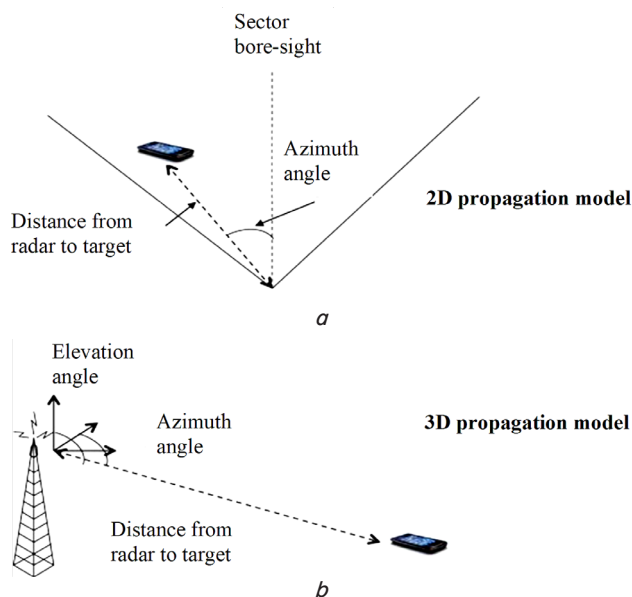


Fig. 1. Radio propagation [10]: *a* – 2D model; *b* – 3D model

By simulating a radar antenna, the effort aims to understand how the performance of radio wave propagation might be affected by the weather. Additionally, it will show how much radar performance may suffer from fog, rain, and other meteorological factors. Looking at the attenuations brought on by the various weather situations should make it simpler to come up with solutions to assist make up for the losses. Losses must be considered while designing antennas since they will have an impact on how well they work in the real world.

2. Literature review and problem statement

Several approaches have been developed to analyze various effects on RF propagation. As previously indicated, radar structures based on Wi-Fi signal interference and modulator designs with excellent spatial efficiency exploiting quantum characteristics of light with a multi-level diffraction (MPD) design have recently been demonstrated. The paper [1] developed next-generation sensors that use direct cellular signal interference and radio frequency rates that benefit from MPD's

high spatial efficiency, but this system cannot be used for other reasons in radar system simulation. The study [2] depended not only on the accuracy of simulation results for radar and target models, but also on radio frequency (RF) environment models for clutter, multi-path, and diffraction. In the simulation of radar functions, all of these elements were regarded as a single scheme propagation component, which provides only a little information on radar models. To imitate the signal intensity of radar systems, a dependable RF environment must be required as in the study [3], which demonstrated various ways for improving the accuracy and reliability of urban localization for highly automated driving. Although the research lowers the error budget of individual sensors by integrating a low-cost GNSS system with visual distance measurement, radar, and 3D mapping data in a complex sensor fusion algorithm, it didn't discuss the Propagation Losses (PL) due to snow, and rain over frequency changes. The paper [4] offered a Cramér-Rao Minimum Analysis investigation on antenna properties over a mono-static multiple-input-multiple-output (MIMO) radar for target tracking techniques. Although the study demonstrated that using distributing the energy transmitted across multiple frequency ranges, a more accurate estimation can be obtained due to frequency diversity, and the detrimental impacts of radiation pattern deviation can be avoided. The research [5] focused on the dynamic impacts of flying on radar cross-section models in aircraft. Her research was based on flight data from three distinct aircraft: a Piper PA-28 Archer II, a Boeing 737, and a Saab JAS 39 Gripen. This study used a simulator with viewing angles towards a radar station positioned in an extension of the desired flight route. However, the study didn't discuss the performance of radio frequency propagation of a radar system over different environmental effects. Correspondingly, the study [6] looked at the capacity of continuous dual-wave (CW) Doppler radar to detect range (RD) for small and rapid targets with high-band resolution. The study recommended that the range accuracy be determined by the processing integration time of the received signal and the velocity of the target. However, they used a limited number of transmitters, making it impossible to collect additional findings and capabilities to learn more about the targets. The researchers [14] exploited targeted geographical variety to boost detection performance to create the best detector in terms of Neyman-Pearson and its analysis for MIMO statistical radar. However, the study also didn't discuss the performance of radio frequency propagation of a radar system over different environmental effects.

When constructing wireless communications systems, constant and reliable communication between antennas is essential. It is crucial to comprehend the potential effects of the antenna's surroundings on the radio waves it transmits. Radio wave propagation can be impacted by a variety of causes, including ionospheric abnormalities. All this allows us to argue that it is appropriate to conduct a study devoted to analyzing the performance of radio frequency propagation of a radar system by analyzing various environmental effects such as Propagation Losses (PL) due to each atmosphere, precipitation, snow, rain, clouds, fog, atmospheric lensing and absorption, and polarization mismatch.

3. The aim and objectives of the study

The aim of the study is to identify some regularities of radio frequency propagation of a radar system by analyzing different environmental effects.

To achieve this aim, the following objectives are accomplished:

- to analyze Free Space Path Loss (FSPL) over range and frequency variation;
- to obtain the relationship between the Propagation Losses (PL) due to each snow, and rain over frequency changes;
- to obtain the relationship between the PL due to fog over frequency changes;
- to analyze the effect of atmospheric gas on RF signal attenuation at a particular altitude against frequency variations;
- to observe the performance of the propagation factor against the antenna range for L-bands and C-band.

4. Materials and methods

4.1. Object and hypothesis of the study

This study identifies some regularities of radio frequency propagation of a radar system by analyzing different environmental effects. This can be achieved by analyzing FSPL over range and frequency variation, obtaining a relationship between the PL due to each snow, and rain with frequency changes, obtaining a relationship between the PL due to fog and frequency changes, analyzing the effect of atmospheric gas on RF signal attenuation, and observing the performance of the propagation factor against the antenna range for L-bands and C-band.

It is assumed that the power value of the received signal (P_r) for mono-static radar can be represented by its range formula:

$$P_r = \frac{P_t G^2 \sigma \lambda^2}{(4\pi)^2 R^4 L}. \quad (1)$$

The parameters P_t , G , σ , R and λ are the power transmitted, the gain of the antenna, the radar cross section (RCS) of a target, the propagation distance, and the wavelength. P_r is inversely proportional to R^4 . The L term includes every PL other than FSPL. This work demonstrates calculating the L term in various contexts. It also includes simulating a variety of RF propagation effects such as multipath propagation of ground bounces, gas in the atmosphere, fog, attenuation due to rain, and free space path loss. The key evaluation here is founded on the series of references «International Telecommunication Union's ITU-R-P», which deals the radio wave propagation and communications.

To simplify the adopted work understanding, the main topic is divided into calculating FSPL, and discussing the variation of PL due to atmosphere, precipitation, snow, rain, clouds, fog, atmospheric lensing, absorption, and polarization mismatch. The study also discusses the vertical coverage diagram and radar propagation factor.

4.2. Calculation of free space path loss (FSPL)

Free Path loss can be calculated in terms of frequency and propagation distance. An RF signal propagates at light speed in free space in every direction. The source of radiation appears as a point in space at a sufficient distance and the produced wave shapes a sphere with a power density inversely proportional to R^2 and a radius equal to R :

$$\frac{P_t}{4\pi R^2}. \quad (2)$$

The open space path loss, also known as the spreading loss, is a loss associated with this propagation method. FSPL is a function of frequency in a quantitative sense, as shown by [5]:

$$L_{fs} = 20 * \log_{10} \left(\frac{4\pi R}{\lambda} \right) \text{dB}. \quad (3)$$

The convention of propagation losses is suitable to obtain the 2-way FSPL through repetition of 1-way FSPL.

4.3. Propagation losses (PL) due to atmosphere and precipitation

Because signals do not all time pass through a vacuum, FSPL only accounts for a portion of signal attenuation. A radio signal interacts with loss energy and airborne particles over propagation paths. The amount of PL changes depending on the density of the water, temperature, and pressure.

4.3.1. Propagation losses (PL) due to snow and rain

Snow and rain can be a serious stumbling block on a radar system, particularly when working at frequencies higher than 5 GHz. Rain is defined by the rain rate, which is measured by (mm/h) according to the International Telecommunication Union (ITU) system [15]. The rain rates are specified as more than 50 mm/h for heavy rains and less than 0.25 mm/h for low rain rates [16]. Rain PL is also proportional to the rain's comparative size to the wavelength of the radio signal and the signal polarization due to the shape of the raindrop. Generally, horizontal polarization is the worst-case scenario for rain-induced PL.

4.3.2. Loss due to clouds and fog

Water droplets also generate clouds and fog; however, they are considerably smaller than raindrops. Fog droplets are typically smaller than 0.01 cm in diameter. The density of liquid water in fog is frequently used to describe it. The liquid water density of a medium fog is 0.05 g/m³ by 300 meters of visibility. The water liquid with a visibility of 50 meters and a density is roughly 0.5 g/m³ during severe fog. The ITU model includes the atmosphere temperature in Celsius for PL due to clouds and fog [17].

4.3.3. Propagation losses due to atmospheric lensing and absorption

The environment is filled with substances that impact signal propagation even when there is no rain or fog. The ITU-based model [18] calculates the attenuation of atmospheric gas relative to both water vapor density, which is measured in g/m³, and dry air pressure, which is measured in hPa for oxygen.

We considered the model «Mean Annual Global Reference Atmosphere» (MAGRA) to calculate PL due to atmospheric absorption and obtain typical values of water vapor density, pressure, and temperature at a given height. It is also possible to specify a latitude model to employ a model that is customized to a specified latitude range.

4.4. Propagation losses due to polarization mismatch

Some kinds of PL, such as rain losses, are reliant on the transmitted signal polarization of RF waves. This is due to the medium's structural and chemical features. In free space, there is PL due to mismatching between the receiving antenna's polarization and the propagated polarization vectors. If the antenna receives polarization orthogonal to the polarization vector of the propagated signal, in which there might be no signal energy possible to receive directly. Because the propagation direction must be considered, the polarization vector of the propagated signal is not always the same as the polarization vectors of the transmitted signal.

4. 5. Vertical coverage diagram and radar propagation factor

A Blake chart (vertical coverage graph) is the concise means of presenting contours of preset power signals as a function of elevation angle and propagation range. Only the vertical plane is taken into account, where both indirect and direct path signals propagate.

Multipath due to ground bounce beside atmosphere refraction produces radiation patterns for a known band that are able to be substantially unlike the supposed broadcast pattern while transmitting above an extensive angle or due to an antenna near the land. The propagation factor of the radar, which is defined as the ratio of the field strength in free space to the actual field strength captures this. As the corresponding phase between the indirect and direct paths of signals varies, the propagation factor might fluctuate dramatically.

4. 6. Vertical coverage diagram and radar propagation factor

A MATLAB-based function called (radarvcd) accepts frequency bands as input and goes back to the range where the received energy in multi-path surroundings equals that in open space. On a range-height-angle chart, this effective range is displayed. This may easily provide the real range recognition for a known free-space detection frequency band as a function of elevation angle, height, and range.

5. Results of the analyzed propagation of a radar system

5. 1. Results of calculating free space path loss

FSPL for the frequency range (1–1,000) GHz using the above equation is shown in Fig. 2.

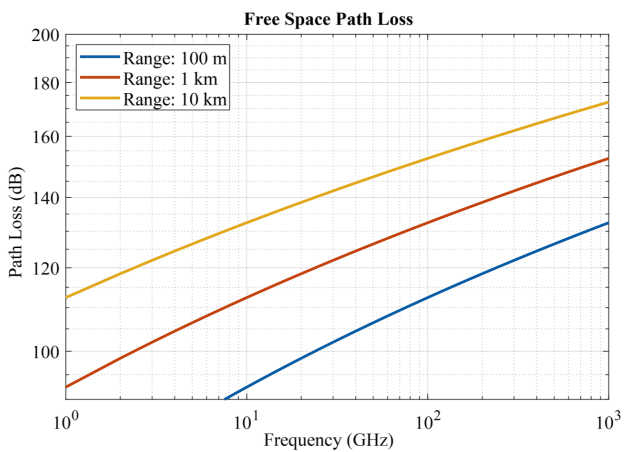


Fig. 2. Free space path loss (FSPL) over frequency change (1–1,000) GHz

The propagation loss increases with range and frequency, as shown in the graph.

5. 2. Propagation losses due to snow and rain

According to the Crane and ITU models, we calculate the PL due to rain in the range (1 GHz–1 THz) with horizontal polarization and zero tilt angles. We assume that the signal propagates in parallel to the ground with zero elevation angle. The simulation parameters to calculate PL for Crane and ITU models are listed in Table 1. Three levels of rain rates (light, moderate, and heavy) are calculated for Crane and ITU mo-

del to demonstrate the attenuation at 5 km over frequency variations as shown in Fig. 3.

Table 1

Simulation parameters for calculating PL for Crane and ITU models

Properties	Rain	Snow	Fog
Range	5 km range	1 km range	$T=15$ degree Celsius
Rain/Snow rate in mm/h	[1 4 20]	[0.1 1.5 4]	Water density=[0.01 0.05 0.5] liquid water density in g/m^3
Frequency range	1 GHz–1 THz	$(1:20)*1e9$	10 GHz–1 THz
Elevation	0		Not applicable
Horizontal polarization	0		Not applicable

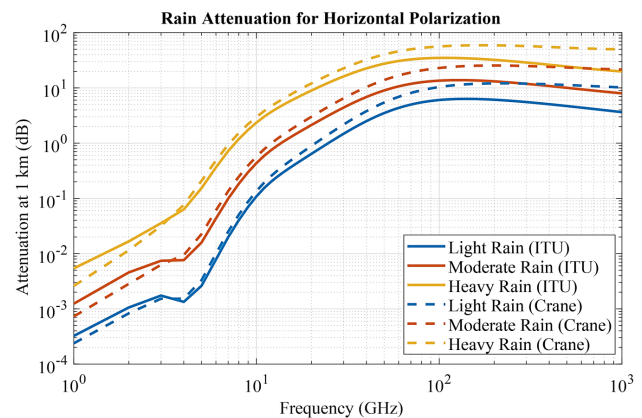


Fig. 3. Rain attenuation for horizontal polarization for three different rain rates

Snow, like rain, can have a substantial impact on the propagation of radio waves. Although this technique tends to miscalculate the PL a little, treating rainfall as snow and computing the PL according to the model of rain is a typical practice. Based on the Gunn-East attenuation model over a frequency of 20 GHz, the PL vs. frequency changes is shown in Fig. 4.

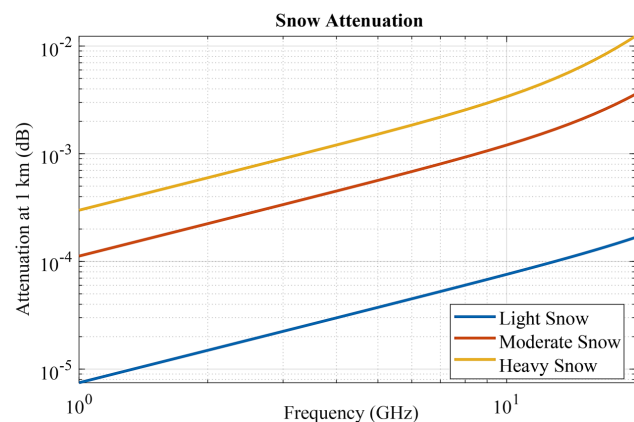


Fig. 4. Snow attenuation vs frequency changes with three different snow rate levels

The frequency of attenuation owing to propagation during snow is greatly reliant on frequency, but not on polarization. Instead of volume, the comparable liquid content is used to parameterize the snow loss model. Snow requires roughly ten times the volume of rain for the same amount of water content.

5.3. Loss due to clouds or fog

PL vs. frequency (10 GHz–1 THz) is plotted for the ITU model for the attenuation caused by fog as shown in Fig. 5.

It’s worth noting that while it’s raining, there’s usually no fog.

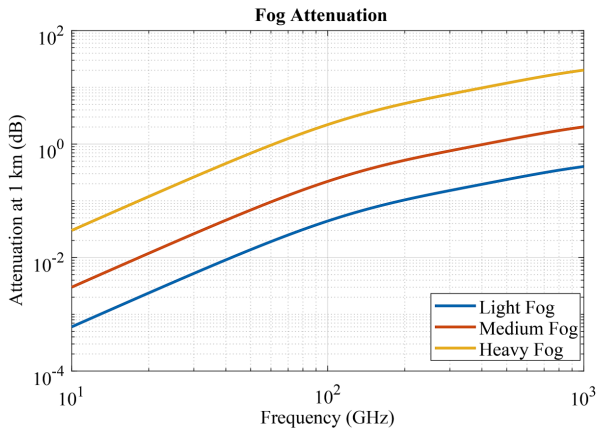


Fig. 5. Attenuation at 1 km vs frequency for International Telecommunication Union model for the attenuation caused by the fog of three rate levels

5.4. Propagation losses due to atmospheric lensing and absorption

We compute the PL for a (–5) degree depressed propagation route (elevation angle) and a 1 km altitude. The calculation of the air absorption total PL along the slanted propagation path excludes the lensing (refraction dissipation). We contrast and compare the PL of high, mid, and low latitude models as shown in Fig. 6.

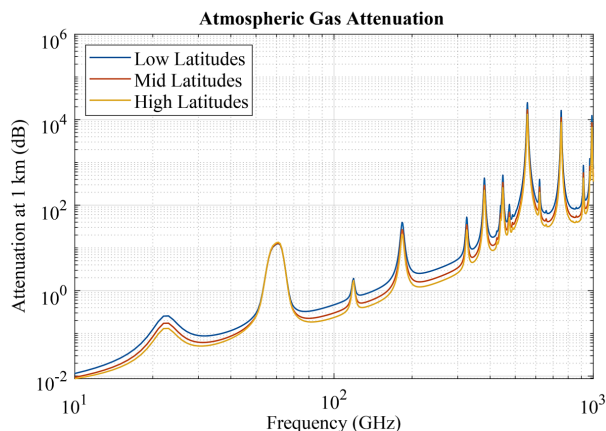


Fig. 6. Atmospheric gas attenuation at (1 km) over frequency variations

With atmospheric pressure, altitude, and consequently refractivity is changed. As a result, the propagation path elevation angle is sufficient to compute PL owing to that result for a particular height. The drawing shows radiation sources with and without refraction as shown in Fig. 7.

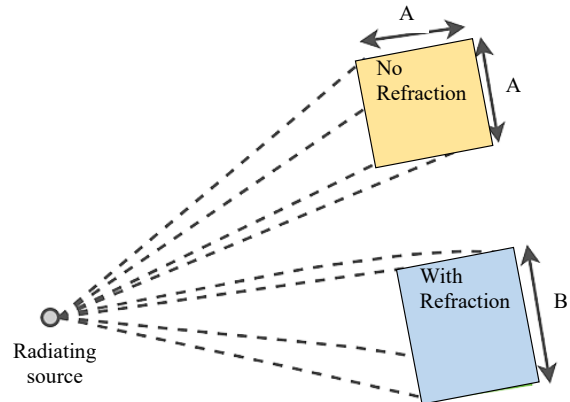


Fig. 7. Radiation source with and without refraction

To calculate PL against frequency, a MATLAB function named (lenspl) is utilized. We plot the PL along with the propagation band for a range of heights because this loss is frequency-independent. For a slanted propagation path, we choose a 0.05° elevation angle. The result under these conditions is shown in Fig. 8.

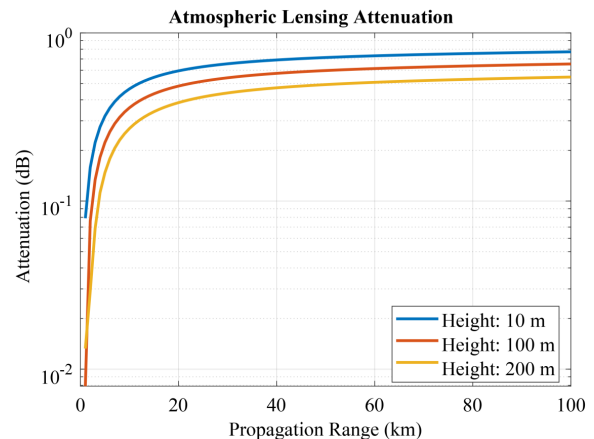


Fig. 8. Atmospheric lensing attenuation against propagation range on different heights

As altitude rises, the amount of lensing attenuation decreases. Lensing attenuation is also offered as secondary output for convenience.

5.5. Vertical coverage diagram and radar propagation factor

We apply 100 km as a detection range in free space, (5.7e9) C-band and 1.06e9L-band transmit frequencies, and a height of 12 m for the antenna using a *sinc* transmit pattern as shown in Fig. 9.

A MATLAB-based function called (radarpropfactor) is considered to calculate the propagation factor for a range interval and compare the two zones.

We calculate the propagation factor at a 1-kilometer preset altitude over the plane and 50–200 kilometers as a propagation range. To depict a smooth surface, we set the height standard deviation and surface slope to zero. The analysis of the two frequency bands separately is shown in Fig. 10.

In the interference zone, it is observed that the propagation factor oscillates, and then rapidly drops in the diffraction zone.

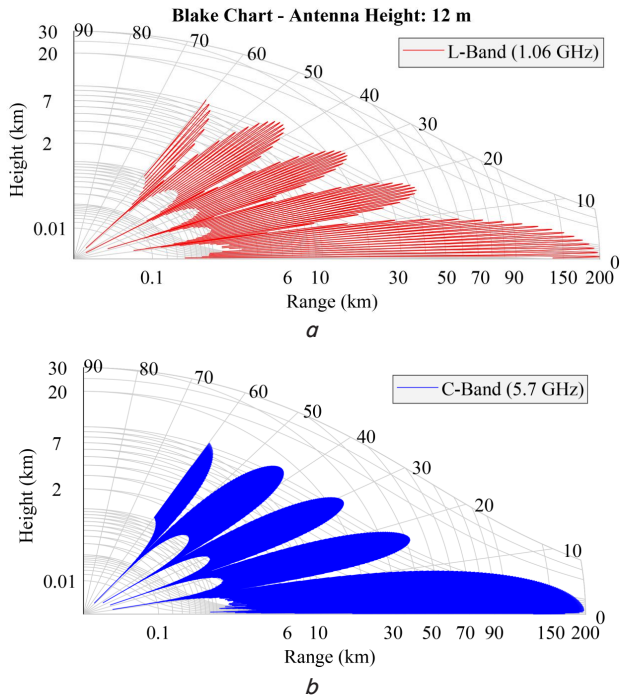


Fig. 9. Blake chart with 12 m height of the antenna: *a* – L-band with 1.06 GHz; *b* – C-band with 5.7 GHz

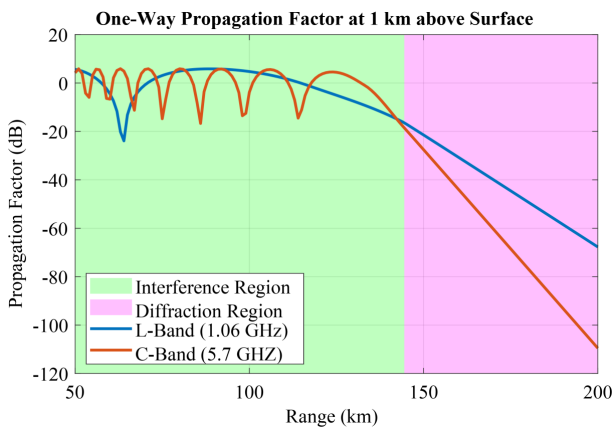


Fig. 10. Propagation factor against the antenna range for L-bands and C-band

6. Discussion of the results of the radio frequency propagation of a radar system

The results obtained from the calculation of Free Space Path Loss (FSPL) against frequency change show that the propagation losses (PL) increase with range and frequency, as shown in Fig. 2. The analysis of the rain attenuation for horizontal polarization for three different rain rates shows that at this propagation range, the PL estimated with the ITU model is generally smaller than the losses computed with the Crane model as depicted in Fig. 3. The ITU model may produce a lower attenuation result than Crane at lower frequencies and narrower propagation ranges. It's worth noting that the models are sufficiently different than at superior frequencies. For a specific model, light rainfall has possibly the same attenuation as moderate rainfall. It is found that snow, like rain, can have a substantial impact on the propagation of radio waves. Although this tends to miscalculate

the PL a little, treating rainfall as snow and computing the PL according to the model of rain is a typical practice. The frequency of attenuation owing to propagation during snow was greatly reliant on frequency, but not on polarization. Instead of volume, the comparable liquid content was used to parameterize the snow loss model. Snow required roughly ten times the volume of rain for the same amount of water content. The PL against frequency changes is proved based on the Gunn-East attenuation model over a frequency of 20 GHz and shown in Fig. 4.

The result of analyzing the attenuation at 1 km vs. frequency variations shows that at roughly 60 GHz, the plot indicates a high absorption owing to air gases, as depicted in Fig. 6. Atmospheric lensing is another cause of losses due to the atmosphere. Due to a refractivity gradient, this is a phenomenon in which the angular extent of a transmission increases with range. The energy density along the nominal (straight) propagation channel falls as a result of this spreading of energy, regardless of frequency.

It is found that as altitude rises, the amount of lensing attenuation decreases. This is shown when computing and plotting the atmospheric lensing attenuation against propagation range on different heights in Fig. 8. It is also found when computing and drawing the relationship between the attenuation of the mismatching polarization along with roll angle changes that at a 90° roll angle, the attenuation approaches infinity. Finally, the relation result between the propagation factor against the antenna range for L-bands and C-band showed that, in the interference zone, the propagation factor oscillates, and then rapidly drops in the diffraction zone as indicated in Fig. 10.

The disadvantage of the presented study is that we didn't discuss the target performance on the wideband channel over a variety of target heights. In addition, the effect of multipath fading with the height of the target is recommended for future work.

7. Conclusions

1. Analysis of Free Space Path Loss (FSPL) shows that the propagation losses (PL) increase linearly with range and frequency when testing FSPL over the frequency range (1–1,000) GHz.

2. The calculation of Propagation Losses (PL) due to rain shows that the attenuation with the ITU model is generally smaller than the losses computed with the Crane model. The ITU model may produce a lower attenuation result than Crane at lower frequencies and narrower propagation ranges. For a specific model, light rainfall has possibly the same attenuation as moderate rainfall. In contrast, the PL due to snow shows that the frequency of attenuation owing to propagation during snow is greatly reliant on frequency, but not on polarization. Instead of volume, the comparable liquid content is used to parameterize the snow loss model. Snow requires roughly ten times the volume of rain for the same amount of water content.

3. The relationship between PL due to fog and frequency change (10 GHz–1 THz) for three fog level densities shows that the wave attenuation is directly proportional to the frequency increase, and the higher fog rate has a higher attenuation pattern.

4. Analyzing the effect of atmospheric gas on RF signal attenuation at 1 km altitude against frequency variations shows that at some frequencies like 60 GHz, the plot

indicates a high absorption owing to air gases. Atmospheric lensing is another cause of losses due to the atmosphere when testing under three levels of height (10 m, 100 m, and 200 m). Due to a refractivity gradient, this is a phenomenon in which the angular extent of a transmission increases with range. The energy density along the nominal (straight) propagation channel falls as a result of this spreading of energy, regardless of frequency.

5. It is observed that the propagation factor oscillates, and then rapidly drops in the diffraction zone when discussing

the propagation factor against the antenna range for L-bands and C-band in the interference zone after the 140 km range.

Conflict of interest

The authors declare that they have no conflict of interest in relation to this research, whether financial, personal, authorship or otherwise, that could affect the research and its results presented in this paper.

References

- Alotaibi, S. (2018). Improved Performance of Doppler Tolerant Radars Using Digital Code. *Journal of Engineering and Applied Sciences*, 1–6. <https://doi.org/10.5455/jeas.2018050101>
- Faruk, N., Abdurashheed, I. Y., Surajudeen-Bakinde, N. T., Adetiba, E., Oloyede, A. A., Abdulkarim, A., Sowande, O., Ifijeh, A. H., Atayero, A. A. (2021). Large-scale radio propagation path loss measurements and predictions in the VHF and UHF bands. *Heliyon*, 7 (6), e07298. <https://doi.org/10.1016/j.heliyon.2021.e07298>
- Faruk, N., Popoola, S. I., Surajudeen-Bakinde, N. T., Oloyede, A. A., Abdulkarim, A., Olawoyin, L. A., Ali, M., Calafate, C. T., Atayero, A. A. (2019). Path Loss Predictions in the VHF and UHF Bands Within Urban Environments: Experimental Investigation of Empirical, Heuristics and Geospatial Models. *IEEE Access*, 7, 77293–77307. <https://doi.org/10.1109/access.2019.2921411>
- De Beelde, B., Plets, D., Desset, C., Tanghe, E., Bourdoux, A., Joseph, W. (2021). Material Characterization and Radio Channel Modeling at D-Band Frequencies. *IEEE Access*, 9, 153528–153539. <https://doi.org/10.1109/access.2021.3127399>
- Fono, V. A., Talbi, L., Safia, O. A., Nedil, M., Hettak, K. (2020). Deterministic Modeling of Indoor Stairwells Propagation Channel. *IEEE Antennas and Wireless Propagation Letters*, 19 (2), 327–331. <https://doi.org/10.1109/lawp.2019.2961641>
- Xing, Y., Rappaport, T. S., Ghosh, A. (2021). Millimeter Wave and Sub-THz Indoor Radio Propagation Channel Measurements, Models, and Comparisons in an Office Environment. *IEEE Communications Letters*, 25 (10), 3151–3155. <https://doi.org/10.1109/lcomm.2021.3088264>
- Vertatschitsch, L. E., Sahr, J. D., Colestock, P., Close, S. (2011). Meteoroid head echo polarization features studied by numerical electromagnetics modeling. *Radio Science*, 46 (6). Portico. <https://doi.org/10.1029/2011rs004774>
- Alslaimy, M., Smith, G. E. (2019). Cramér-Rao lower bound for ATSC signal-based passive radar systems. *Electronics Letters*, 55 (8), 479–481. Portico. <https://doi.org/10.1049/el.2019.0011>
- Shijer, S. S., Sabry, A. H. (2021). Analysis of performance parameters for wireless network using switching multiple access control method. *Eastern-European Journal of Enterprise Technologies*, 4 (9 (112)), 6–14. <https://doi.org/10.15587/1729-4061.2021.238457>
- Al-Shoukry, S., M. Jawad, B. J., Musa, Z., Sabry, A. H. (2022). Development of predictive modeling and deep learning classification of taxi trip tolls. *Eastern-European Journal of Enterprise Technologies*, 3 (3 (117)), 6–12. <https://doi.org/10.15587/1729-4061.2022.259242>
- Hultell, J., Johansson, K. (2006). Performance Analysis of Non-Cosited Evolved 2G and 3G Multi-Access Systems. 2006 IEEE 17th International Symposium on Personal, Indoor and Mobile Radio Communications. <https://doi.org/10.1109/pimrc.2006.254249>
- Aytekin, A., Gulbahar, B. (2020). Experimental Analysis of RF based Multi-plane-diffraction with Over-the-air Active Cellular Signal Measurements. 2020 28th Signal Processing and Communications Applications Conference (SIU). <https://doi.org/10.1109/siu49456.2020.9302221>
- Quanmin, W., Chuncai, W., Gang, G., Kedi, H. (2010). RF Effect Algorithms of Terrain Environment in Signal-Level Radar System Simulation. 2010 Second International Conference on Computer Modeling and Simulation. <https://doi.org/10.1109/iccms.2010.96>
- Kang, S., Oldenburg, D. W., Heagy, L. J. (2019). Detecting induced polarisation effects in time-domain data: a modelling study using stretched exponentials. *Exploration Geophysics*, 51 (1), 122–133. <https://doi.org/10.1080/08123985.2019.1690393>
- ITU-R P.838-3. Specific attenuation model for rain for use in prediction methods. Available at: https://www.itu.int/dms_pubrec/itu-r/rec/p/R-REC-P.838-3-200503-1!!PDF-E.pdf
- Armon, M., Marra, F., Enzel, Y., Rostkier-Edelstein, D., Garfinkel, C. I., Adam, O., Dayan, U., Morin, E. (2021). Reduced Rainfall in Future Heavy Precipitation Events Related to Contracted Rain Area Despite Increased Rain Rate. *Earth's Future*, 10 (1). Portico. <https://doi.org/10.1029/2021ef002397>
- ITU-R P.840-5. Attenuation due to clouds and fog. Available at: https://www.itu.int/dms_pubrec/itu-r/rec/p/R-REC-P.840-5-201202-S!!PDF-E.pdf
- ITU-R P.676-10. Attenuation by atmospheric gases. Available at: https://www.itu.int/dms_pubrec/itu-r/rec/p/R-REC-P.676-10-201309-S!!PDF-E.pdf